Analysis of the Hyperfine-Shifted Nitrogen-15 Resonances of the Oxidized Form of *Anabaena 7120* Heterocyst Ferredoxin†

Young Kee Chae and John L. Markley*

Graduate Program in Biophysics and Department of Biochemistry, University of Wisconsin-Madison, Madison, Wisconsin 53706

Received April 28, 1994; Revised Manuscript Received October 6, 1994®

ABSTRACT: Hyperfine-shifted nitrogen signals have been detected in one-dimensional ^{15}N NMR spectra of oxidized *Anabaena 7120* heterocyst ferredoxin labeled uniformly with ^{15}N. Several of these have been classified by amino acid type by reference to results from selective ^{15}N-labeling studies. Remarkable agreement is seen between a dipole−dipole analysis of the ^{15}N T_1 relaxation and the distances of several of the nitrogens from the irons of the cluster as derived from the X-ray structure of this protein [Jacobson, B. L., Chae, Y. K., Markley, J. L., Rayment, I., & Holden, H. M. (1993) *Biochemistry 32,* 6788−6793]. The agreement is within experimental error for hyperfine-shifted nitrogens that are at least 4.2 Å distant from either of the irons of the cluster; however, the simple model appears to fail for hyperfine-shifted nitrogens that are closer to the cluster. The failure of the model for short distances may stem either from a breakdown of the point−dipole approximation and/or from neglect of delocalization of unpaired electron density from the iron ions to other atoms. Even with the above limitations, dipolar analysis of ^{15}N relaxation should provide useful distance constraints for solution-state studies of iron−sulfur proteins.

In NMR[1] spectra of ferredoxins, several broad resonances can be found outside the diamagnetic region. Such resonances originate from coupling between the nuclear spins and the unpaired electron spin through contact or pseudocontact mechanisms (Webb, 1970). Since the line widths of pseudocontact shifted signals are proportional to the square of the magnetogyric ratio (Bloembergen & Morgan, 1961), nitrogen-15 resonances are affected about 100-fold less than hydrogen-1. Therefore, ^{15}N spectra provide much better resolution than ^{1}H spectra in the hyperfine-shifted territory and offer a useful window for investigations of residues close to paramagnetic groups (Oh & Markley, 1990). In spite of this advantage, hyperfine-shifted ^{15}N resonances have not attracted much attention. A few years ago, nine hyperfine-shifted ^{15}N resonances were reported for the vegetative ferredoxin from *Anabaena 7120* (Oh & Markley, 1990), but no assignments were made. More recently, one of these peaks was assigned to arginine-42, and four others were assigned tentatively to the four cysteines that ligate the cluster (Cheng et al., 1994).

We present here a partial analysis of the hyperfine-shifted region of the ^{15}N NMR spectrum of *Anabaena 7120* heterocyst ferredoxin in its oxidized state. The heterocyst ferredoxin (Böhme & Haselkorn, 1988), which is involved in electron transport in nitrogen fixation, has 51% sequence identity to the vegetative ferredoxin (Ho et al., 1979), which is involved in photosynthetic electron transport. Amino acid selective ^{15}N labeling has been employed in order to lower the ambiguity of the assignments. Comparison of T_1 relaxation data for the nitrogen resonances with the X-ray structure (Jacobson et al., 1993) suggests that electron-nuclear dipole−dipole interactions provide the dominant relaxation mechanism for most of the ^{15}N nuclei that show hyperfine shifts.

MATERIALS AND METHODS

Sample Preparation. The protein was expressed heterologously in *Escherichia coli*, reconstituted, and purified as described by Jacobson et al. (1992). Protein samples were labeled uniformly with ^{15}N by growing the expression host BL21(DE3) on [99% ^{15}N]NH_4Cl as the sole nitrogen source (Chae et al., 1994). Additional samples were labeled selectively with ^{15}N by incorporating ^{15}N-labeled amino acids (Chae et al., 1994). Individual samples studied here contained [^{15}N]Gly, [^{15}N]Gly + [^{15}N]Ser, [^{15}N]Cys, or [^{15}N]Leu. ^{15}N uniformly labeled, [^{15}N]Gly, and [^{15}N]Gly + [^{15}N]Ser selectively labeled *Anabaena 7120* vegetative ferredoxin samples were prepared in the same way. All NMR samples consisted of 3−5 mM protein in 20 mM phosphate buffer at pH 7.5; the solvent contained 10% $^{2}H_2O$ to provide an NMR lock signal.

NMR Spectroscopy. Data were recorded at 298 K on a Bruker AM-600 or DMX-600 NMR spectrometer with a 5-mm reverse probe or a 5-mm broad-band probe. No proton decoupling was used in any of the experiments: protons attached to hyperfine-shifted nitrogens are effectively decoupled as a result of their rapid relaxation caused by the paramagnetic cluster. A short relaxation delay (total recycling time <400 ms) was used in order to enhance resonances from the hyperfine shifted nitrogens and to suppress those from diamagnetic nitrogens. T_1 relaxation times were measured by means of the conventional inversion−recovery

† This work was supported by NSF Grant MCB-9215142 and USDA/SEA Grant 9200684. NMR studies were carried out in the National Magnetic Resonance Facility at Madison, which is supported by NIH Grant RR02301. Equipment in the NMR Facility was purchased with funds from the NIH Biomedical Research Technology Program (Grant RR02301), the University of Wisconsin, the NSF Biological Instrumentation Program (Grant DMB-8415048), NIH Shared Instrumentation Program (Grant RR02781), and the U.S. Department of Agriculture.

* To whom correspondence should be addressed.

® Abstract published in *Advance ACS Abstracts,* December 1, 1994.

[1] Abbreviations: NMR, nuclear magnetic resonance; d_r, reduced distance (see eq 3); 1D, one dimensional; 2D, two dimensional; 3D, three dimensional.

0006-2960/95/0434-188$09.00/0

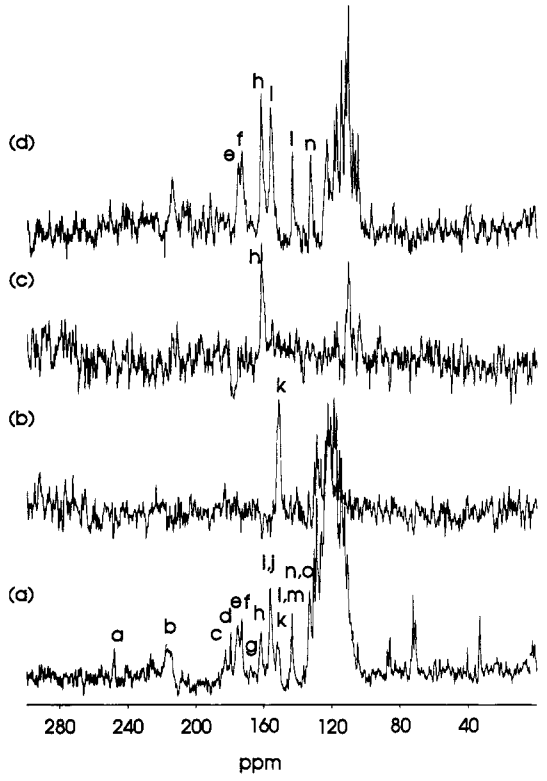

FIGURE 1: One-dimensional nitrogen-15 NMR spectra of various ^{15}N-labeled samples of oxidized *Anabaena 7120* heterocyst ferredoxin: (a) uniformly ^{15}N-labeled, (b) labeled selectively with [^{15}N]-Leu, (c) labeled selectively with [^{15}N]Gly, and (d) labeled selectively with [^{15}N]Gly + [^{15}N]Ser.

pulse sequence (180°$-\tau$(delay)$-$90°) (Vold et al., 1968); the simple 180° pulse was replaced by a composite 180° pulse (Freeman et al., 1980).

NMR Data Processing and Curve Fitting. NMR data were processed on Silicon Graphics (Mountain View, CA) workstations with FELIX (Biosym, San Diego, CA) software. The typical sizes of the raw data sets were 4K or 8K, and the typical spectral width was over 300 ppm. After application of a line broadening factor of 20$-$30 Hz, the data sets were zero-filled to 4K$-$16K. Then each data set was Fourier transformed, phased, and baseline corrected. ^{15}N chemical shifts were referenced to external [^{15}N]acetylglycine, by assuming that the nitrogen frequency of the [^{15}N]acetylglycine was at 120.0 ppm from liquid ammonia. T_1 relaxation data were fitted to

$$M(\tau) = M_0[1 - 2\exp(-\tau/T_1)] \quad (1)$$

where M_0 and T_1 are the parameters to be fitted and $M(\tau)$ is the experimental intensity of the resonance investigated at delay time τ. The Sigma Plot 5.0 (Jandel Scientific, Corte Madera, CA) software package was used for curve fitting.

RESULTS AND DISCUSSION

Detection of Hyperfine-Shifted ^{15}N Signals. The optimal recycling time (acquisition time plus relaxation delay time) is one that allows adequate T_1 relaxation of the hyperfine peaks but very little relaxation of the diamagnetic peaks. A figure in the supplementary material demonstrates that a recycling time of about 400 ms provides optimal detection of the hyperfine-shifted ^{15}N signals.

Table 1: Residues on *Anabaena 7120* Heterocyst Ferredoxin Whose Nitrogens Are within 8.5 Å from at Least One of the Iron Atoms in the [2Fe-2S] Cluster

residue	d_1 (Å, Fe_1)[a]	d_2 (Å, Fe_2)[b]	d_r (Å)[c]	d_r^6 (Å^6)
F39	7.06	6.70	6.115	52273
S40	4.63	5.44	4.388	7138
C41	3.67	5.50	3.619	2247
H42	3.73	4.29	3.513	1881
S43	4.47	4.70	4.076	4586
G44	4.29	4.27	3.813	3073
S45	4.27	5.45	4.125	4927
C46	3.52	5.34	3.474	1758
S47	4.83	6.16	4.665	10306
S48	4.73	5.52	4.475	8031
C49	4.96	4.26	4.027	4265
V50	6.94	5.65	5.414	25195
F65	8.12	8.50	7.390	162862
1.77	8.41	6.43	6.238	58908
L78	7.64	5.12	5.047	16527
C79	6.81	4.13	4.097	4729
V80	7.69	5.30	5.211	29918

[a] Distance (d_1) between the nitrogen of the residue and Fe_1 of the X-ray structure (Jacobson et al., 1993). [b] Distance (d_2) between the nitrogen of the residue and Fe_2 of the X-ray structure (Jacobson et al., 1993). [c] Reduced distance. See eq 3 in the text.

Hyperfine-Shifted ^{15}N Resonances. Figure 1a shows the one-dimensional ^{15}N spectrum of *Anabaena 7120* heterocyst ferredoxin in its oxidized state at 298 K. Twelve separate peaks were resolved downfield of the diamagnetic region. Since three of these signals correspond to two overlapped nitrogens, the total number of resonances in this region was 15. These are labeled (a$-$o) in the figures. Peaks a and g were assigned to the N^ϵ and N^δ atoms of H93, respectively, on the basis of a 2D [^{1}H$-^{15}$N] HMQC spectrum (not shown). The remaining 13 signals correspond to hyperfine-shifted ^{15}N resonances.

Residues Close to the Iron$-$Sulfur Cluster. Table 1 lists amino acid residues whose nitrogen atoms are closer than 8.5 Å from one or both irons of the cluster as determined from the X-ray structure of the same protein in the same oxidation state (Jacobson et al., 1993). With one exception, no NMR signals from any of these residues were detected in the normal diamagnetic regions of conventional 2D and 3D NMR spectra (Chae et al., 1994). The exception was L77, some of whose resonances were seen in a 2D [^{1}H$-^{15}$N] HMQC spectrum of a sample selectively labeled with [^{15}N]Leu.

Residues Chosen for Selective Labeling. The region of the protein affected by the paramagnetism includes five serines, four cysteines, two leucines, two valines, two phenylalanines, one histidine, and one glycine (Table 1). Among these residues, serines, cysteines, leucines, and glycines were chosen for selective labeling. Incorporation of [^{15}N]Gly led to labeling of glycines and serines in one sample. Although amino acid auxotrophic strains were not used, none of the other samples showed migration of the label to other amino acid types. Thus, 12 of the 17 candidate residues could be investigated with this set of labeled proteins.

^{15}N Spectra of Selectively Labeled Samples. Figure 1 compares the ^{15}N spectra of samples labeled uniformly with ^{15}N (Figure 1a), selectively with [^{15}N]Leu (Figure 1b), selectively with [^{15}N]Gly (Figure 1c), and selectively with [^{15}N]Gly + [^{15}N]Ser (Figure d). Figure 2 shows expanded views of the hyperfine-shifted regions of the samples labeled

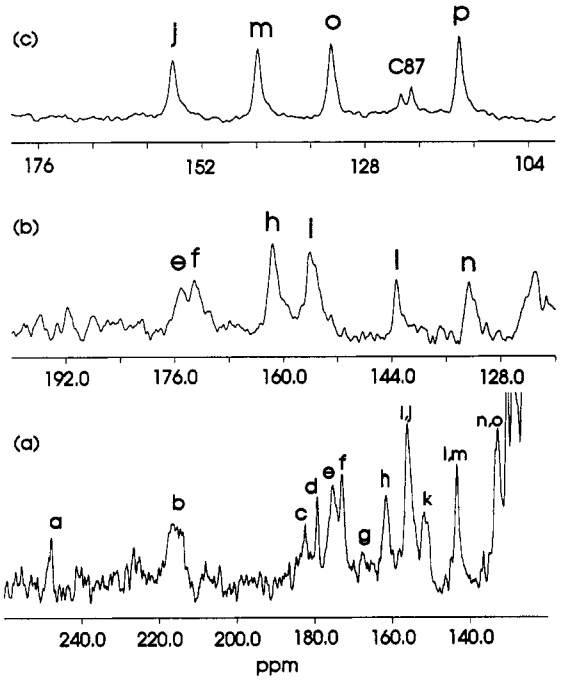

FIGURE 2: Expansions of ^{15}N spectra of oxidized *Anabaena 7120* heterocyst ferredoxin: (a) uniformly ^{15}N-labeled, (b) labeled selectively with [^{15}N]Gly + [^{15}N]Ser, and (c) labeled selectively with [^{15}N]Cys.

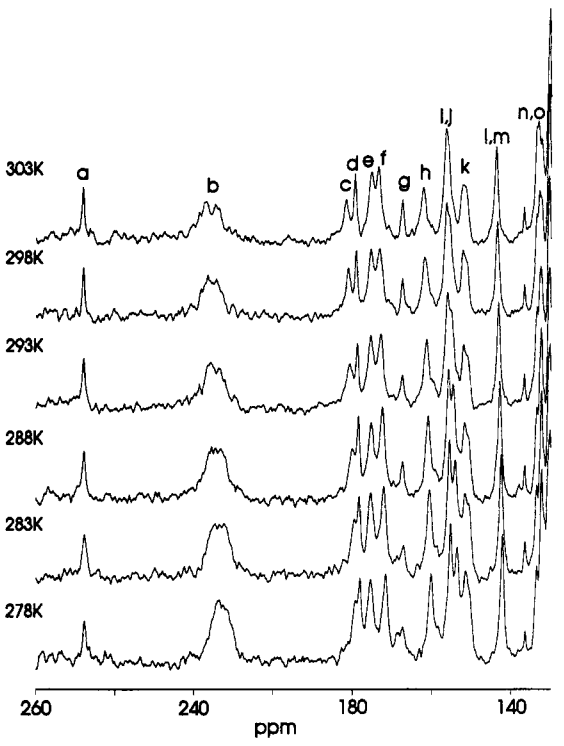

FIGURE 3: Temperature dependence of the ^{15}N NMR spectrum of uniformly ^{15}N-labeled *Anabaena 7120* heterocyst ferredoxin in its oxidized state. Temperature values are given in the figure.

uniformly with ^{15}N (Figure 2a), [^{15}N]Gly + [^{15}N]Ser, and [^{15}N]Cys (Figure 2c). The spectrum of [^{15}N]Gly heterocyst ferredoxin (Figure 1c) contained only one of the 13 hyperfine peaks (h). Thus peak h is assigned to G44, the only glycine that is close to the [2Fe-2S] cluster. By difference (Figure 1d), peaks e, f, i, l, and n must be from serine residues. Similar analysis of the spectrum of a sample of [^{15}N]Leu heterocyst ferredoxin (not shown) revealed that peak k is from one of the two leucines in the molecule (L77 or L78). Thus peak k is assigned to L78 which is closer to the [2Fe-2S] cluster than L77. A very weak peak, with a diamagnetic ^{15}N chemical shift, was seen in the [^{1}H-^{15}N] HMQC spectrum of the [^{15}N]Leu labeled sample (spectrum not shown); it was assigned to L77 according to the above reasoning.

Temperature Dependence of the Hyperfine-Shifted ^{15}N Resonances. All hyperfine-shifted ^{15}N resonances showed anti-Curie-type temperature dependence (Figure 3). Spectra of the sample labeled with [^{15}N]Cys (Figure 2c) showed that peaks i, l, and n, which arise from three of the five serines, overlap at 298 K with cysteine peaks j, m, and o, respectively. Two of the three pairs of peaks are resolved separately at 278 K (i, j, n, and o; Figure 3). However, peaks l and m remained overlapped at all temperatures because they have similar temperature dependences.

Relaxation Time Measurements. Figure 4 shows typical T_1 relaxation data as stacked plots. The results of the T_1 measurements are given in Table 2. The major potential sources of error in the T_1 relaxation time measurements were in the data processing steps following Fourier transformation of the partially relaxed spectra. In order to avoid bias in the intensity measurements, the phasing, baseline correction, and intensity measurements were repeated five times independently with the Felix software, and the average intensity was used.

Tentative Assignments of Hyperfine-Shifted Nitrogen Resonances. According to Bertini and Luchinat (1986), the relationship between the distance from the unpaired electron to the nucleus (d) and the T_1 relaxation time is given by

$$\frac{1}{T_1} = \frac{4}{3}\left(\frac{\mu_0}{4\pi}\right)^2 \frac{\gamma_N^2 g_e^2 \mu_B^2 S(S+1)}{d^6}\tau_c + \frac{2}{3}\left(\frac{A_c}{\hbar}\right)^2 S(S+1)\tau_s + \left(\frac{\mu_0}{4\pi}\right)^2 \frac{4\omega_I^2 g_e^2 \mu_B^4 S^2(S+1)^2}{(3kT)^2 d^6}\tau_c \quad (2)$$

The first, second, and third terms come from the dipolar, contact, and Curie spin relaxation mechanisms, respectively. However, the third term, which arises from the Curie spin relaxation, is always negligible (Bertini & Luchinat, 1986). Thus, only the first two terms of eq 2 need to be considered. Although the second term does not show an explicit distance dependence, the hyperfine coupling constant (A_c) decreases with distance (Bertini & Luchinat, 1986).

For the purpose of analyzing the dipolar component, the unpaired electron was assumed to be localized between the two iron atoms (on average), and the distance between the nucleus and each of the two iron atoms d_1 and d_2 was converted to the reduced distance (d_r) (Oh & Markley, 1990) by means of the equation

$$d_r = [d_1^6 d_2^6/(d_1^6 + d_2^6)]^{1/6} \quad (3)$$

Thus to a first approximation, the dipolar contribution to the T_1 relaxation is proportional to the sixth power of the reduced distance (d_r). In order to evaluate this relaxation model, distances were taken from the X-ray structure (Jacobson et al., 1993). Table 1 contains the X-ray distances between the nitrogen atoms of the residues considered here and the iron atoms of the cluster and the reduced distances derived from them.

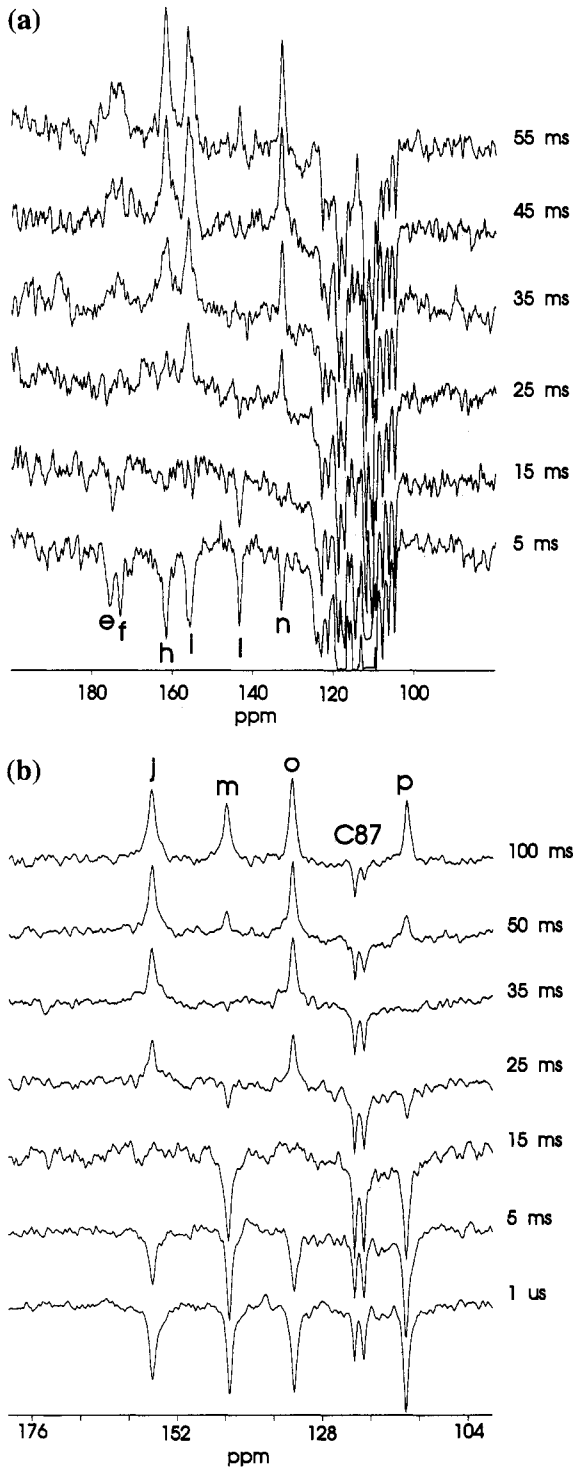

FIGURE 4: Partially relaxed ^{15}N spectra of ^{15}N-labeled samples of oxidized heterocyst ferredoxin obtained with the $180-\tau-90$ pulse sequence: (a) [^{15}N]Gly + [^{15}N]Ser ferredoxin; (b) [^{15}N]Cys ferredoxin. The τ values are given at the end of each trace.

The serine nitrogen resonances were assigned tentatively by ordered pairing of the reduced serine nitrogen to cluster distances and serine nitrogen T_1 values: shorter T_1 with shorter d_r. This pairs peak e with S48, peak f with S40, peak i with S45, peak l with S47, and peak n with S43 (Table 3). The cysteine nitrogen resonances were assigned tentatively by the same method: peak j with C46, peak m with C49, peak o with C41, and peak p with C79 (Table 4).

Table 2: Results of the ^{15}N T_1 Relaxation Time Measurements

peak[a]	type	δ (ppm)[b]	T_1 (ms)	σ (ms)
e	Ser	175.40	37.79	4.29
f	Ser	173.31	34.96	3.14
h	Gly	161.82	26.06	0.90
i	Ser	156.34	21.55	1.42
j	Cys	156.36	20.69	0.75
k	Leu	152.16	77.56	7.36
l	Ser	143.54	47.52	4.04
m	Cys	143.86	50.30	1.49
n	Ser	132.83	19.76	1.00
o	Cys	133.11	20.87	0.66
p	Cys	114.35	53.46	2.20

[a] Peak lettering convention shown in Figure 1. [b] Chemical shift at 298 K from external liquid ammonia (see Materials and Methods).

Table 3: Tentative Assignments of the Serine, Glycine, and Leucine Nitrogen Resonances and Comparison of the Reduced Distances between the Nitrogen Atoms and the Iron–Sulfur Cluster Derived from the X-ray Structure with Those Calculated from the Best Fit of the ^{15}N Relaxation Rates for These Residues

peak	assignments[a]	$d_r^{X\text{-ray}}$ (Å)[b]	d_r^{calc} (Å)[c]	Δd_r (Å)
e	S48	4.475	4.520	0.045
f	S40	4.388	4.459	0.071
i	S45	4.125	4.014	0.021
l	S47	4.665	4.703	0.038
n	S43	4.076	4.044	0.032
k	L78	5.047	5.131	0.084

[a] These assignment results from the assumption that the ^{15}N relaxation rate correlates with proximity to the cluster. Given the errors in the analysis, however, the assignments of peaks e and f could be reversed as could those of peaks i and n. [b] From the X-ray structure (Jacobson et al., 1993). See Table 1. [c] Given by $1/T_1 (\times 10^2) = 2.225/d_r^6 (\times 10^4) + 0.1$ (eq 4 in the text) where T_1 is from Table 2.

Table 4: Speculative Assignments of the Cysteine and Glycine Nitrogen Resonances: Comparison of the Reduced Distances between the Nitrogen Atoms and the Iron–Sulfur Cluster Derived from the X-ray Structure with Those Calculated from the ^{15}N T_1 Relaxation Data

peak[a]	assign-ment[b]	$d_r^{X\text{-ray}}$ (Å)[c]	d_r^{calc} (Å)[d]	Δd_r (Å)[e]	d_r^{calc} (Å)[f]	Δd_r (Å)[g]
j	C46	3.474	3.543	0.069	4.076	0.602
m	C49	4.027	4.130	0.103	4.751	0.724
o	C41	3.619	3.548	0.071	4.082	0.463
p	C79	4.097	4.174	0.077	4.802	0.705
h	G44	3.813	3.686	0.127	4.240	0.427

[a] As defined in Figure 1. [b] These assignments result from the assumption that the ^{15}N T_1 relaxation rate correlates with proximity to the cluster. [c] From the X-ray structure (Jacobson et al., 1993). [d] Calculated from the best fit of eq 2 to the T_1 relaxation data for the four cysteine and glycine nitrogens. [e] Difference between the reduced distances for the X-ray structure and those from the best fit of eq 2 to the T_1 relaxation data for the cysteine and glycine nitrogens. [f] Calculated from the parameters for the best fit of eq 2 to the T_1 relaxation data for the serine and leucine nitrogens. [g] Difference between the reduced distances from the X-ray structure and those calculated from the line for serine and leucine nitrogens.

Analysis of the Relaxation Results. The T_1 data were evaluated by fitting to the equation

$$1/T_1 \times 10^2 = a/d_r^6 \times 10^4 + b \qquad (4)$$

where a and b are adjustable parameters. As seen in Figure 5, the ^{15}N relaxation data from the serines and leucine fall on a straight line (generated from the ordered pairing described above). The fitted values of a and b were 2.402

Table 5: Test against *Anabaena 7120* Vegetative Ferredoxin Data

residue	T_1 (ms)	σ (ms)	$d_r^{X\text{-ray}}$ (Å)[a]	d_r^{calc} (Å)[b]	Δdr (Å)
S40	20.47	0.65	4.503	4.068	0.435
S47	45.03	3.78	4.512	4.659	0.147
G44	24.69	0.90	3.885	3.652	0.233
C41	46[c]	nd	3.581	4.066	0.485
C46	22[c]	nd	3.507	3.580	0.073

[a] From the X-ray structure (Rypniewski et al., 1991; Holden et al., 1994). [b] Calculated from the serine and leucine nitrogen line (Figure 5, solid line) for S40 and S47, and from the cysteine and glycine line (Figure 5, dotted line) for G44, C41, and C46. [c] From Cheng et al. (1994).

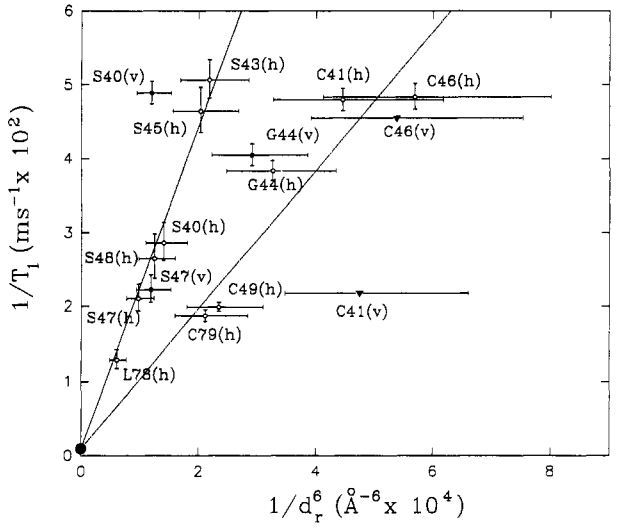

FIGURE 5: Correlation between the inverse sixth power of the reduced distance of a nitrogen atom to the iron–sulfur cluster ($1/d_r^6$) and its longitudinal relaxation rate ($1/T_1$) for various residues of oxidized *Anabaena* 7120 heterocyst ferredoxin [open symbols; extension (h) on residue assignments] and oxidized *Anabaena* 7120 vegetative ferredoxin [closed symbols; extension (v) on residue assignments]. The data were fitted to the equation $1/T_1$ ($\times 10^2$) = a/d_r^6 ($\times 10^4$) + 0.1 (see text). The solid line represents the best fit of the data for the serine and leucine nitrogens of the heterocyst ferredoxin; the dotted line represents the best fit of the data for the cysteine and glycine nitrogens of the heterocyst ferredoxin: The distances were taken from the X-ray structures of the same proteins (Jacobson et al., 1993; Rypniewski et al., 1991; Holden et al., 1994). The assignments assumed are given in Tables 3–4. The error bars represent uncertainties propagated from errors in atom positions from the X-ray structures (± 0.2 Å) and from estimated errors in the experimental ^{15}N T_1 measurements.

(± 0.1059) and −0.2771 (± 0.1601), respectively, for the serine and leucine nitrogens. The y intercept, however, should be positive because it corresponds to the diamagnetic component of the relaxation (the negative value for b probably arises from errors in the T_1 measurements). When the y intercept was fixed at $b = 0.1$ s^{-1} (a typical diamagnetic $1/T_1$ value), a was 2.170 (± 0.05374). This is the line shown in Figure 5.

The excellent fit of the serine and leucine data to this model suggests that these nitrogens are relaxed predominantly by dipolar coupling to electrons. The distances of these nitrogens from the cluster derived from the fitted ^{15}N relaxation data are nearly identical to the x-ray distances (Table 3). The average deviation Δd_r is 0.0485 Å; the largest Δd_r is that for L78 (0.084 Å). All serine and leucine data points (Figure 5) are inside the 95% confidence range from the fitted line. As noted in Table 3, since the experimental relaxation rates for serine peaks e and f and for peaks i and n are within experimental error (Table 2), this approach cannot distinguish the tentative assignments used in the relaxation analysis from assignments in which e and f and/or i and n are reversed.

However, the points for the nitrogens of G44 and all four cysteines lie well off the fitted curve for the serine and leucine data (solid line, Figure 5). These correspond to the nitrogens that are closest to the iron atoms, yet they are not relaxed as strongly with reciprocal sixth-power distance as nitrogens that are farther away. These anomalous nitrogens can be fitted by a separate straight line (dotted line, Figure 5) with the same y-intercept but with $a = 0.9366$ (± 0.6525). The quality of the separate fit for the cysteine and glycine nitrogens (average $\Delta d_r = 0.089$ Å, Table 4) is much lower than that for the serine and leucine nitrogens. These results suggests that the simple dipolar model for ^{15}N relaxation fails with nitrogens that are closer than about 4.2 Å from either of the iron atoms. It may be that at such short distances the dipolar approximation breaks down or that delocalization of electron density from the irons to other atoms cannot be neglected. The latter explanation may account for the anomalous results for the cysteinyl nitrogens since electron delocalization onto various cysteinyl atoms is well documented (Cheng et al., 1994).

According to the X-ray structure (Jacobson et al., 1993), some of the paramagnetically affected nitrogens are involved in hydrogen bonds to the cysteine sulfurs that ligate the [2Fe-2S] cluster. These include S43N to C41S$^\gamma$, S45N to C41S$^\gamma$, S48N to C46S$^\gamma$, and G44N to C79S$^\gamma$. The hydrogen bonding does not seem to affect the T_1 relaxation times of the serine nitrogens since nitrogens that are involved in hydrogen bonding and those that are not fall on the same straight line.

Test of the Model with Nitrogen-15 Relaxation Data for Anabaena 7120 Vegetative Ferredoxin. Cheng et al. (1994) recently measured the T_1 values for the ^{15}N NMR signals from the cysteines of oxidized *Anabaena 7120* vegetative ferredoxin and made fairly firm assignments to one of these by dual ^{15}N and ^{13}C labeling and to another on the basis of its relaxation properties. Additional ^{15}N relaxation measurements (data not shown) were made for G44 (the only glycine near the cluster) and for two serines near the cluster (S40 and S47 whose signals were assigned on the basis of differential relaxation). These data were examined as a test of the dipolar relaxaton model developed above. The X-ray structure of the *Anabaena 7120* vegetative ferredoxin has been solved (Rypniewski et al., 1991) and recently refined to 1.7-Å resolution (Holden et al., 1994). The results are shown as solid symbols in Figure 5. The data point for S47 (vegetative) falls on the solid line; that for S40 (vegetative) is somewhat off the line; and those for the two cysteines, C41 (vegetative) and C46 (vegetative), fall well to the right of the solid line as do the cysteine data for the heterocyst ferredoxin.

CONCLUSION

The nitrogens of the cysteinyl ligands to the cluster exhibit anomalous ^{15}N T_1 relaxation behavior since they clearly fall off the curve that gives a reasonable fit to all the other data points (solid line, Figure 5). These anomalies are seen with data from both ferredoxins studied (*Anabaena* 7120 vegetative and heterocyst). It appears prudent at present to exclude data from the cluster ligands from simple dipolar analysis.

The fact that T_1 relaxation data from the non-cysteinyl, hyperfine-shifted nitrogens can be fitted by a simple dipolar model suggests that such measurements could form the foundation for a new strategy for determining protein structure near paramagnetic centers. It is important, however, that the model be tested with ^{15}N relaxation results from other paramagnetic proteins, particularly with data sets containing assignments made independently from the model. Current methods of calculating NMR structures are highly dependent on the identification of interproton NOEs, but this approach fails with paramagnetic proteins, such as [2Fe-2S] ferredoxins, in which signals from protons within ~6 Å are severely broadened. Distance information from ^{15}N T_1 relaxation times could provide the missing information needed to determine local three-dimensional structure near such paramagnetic centers. Distance bounds developed from ^{15}N T_1 values should be interpreted loosely to account for anomalous effects such as those seen for G44. The addition of ±0.5 Å to each distance bound (d_r) would take care of all variation seen to date and yet provide much better distance estimates than those currently available from hyperfine NOEs.

SUPPLEMENTARY MATERIAL AVAILABLE

One figure showing the one-dimensional nitrogen-15 spectra of [99% UL ^{25}N] *Anabaena 7120* heterocyst ferredoxin (2 pages). Ordering information is given on any current masthead page.

REFERENCES

Bertini, I., & Luchinat, C. (1986) *NMR of Paramagnetic Molecules in Biological Systems*, The Benjamin/Cummings Publishing Company, Inc., Menlo Park, CA.

Bloembergen, N., & Morgan, L. O. (1961) *J. Chem. Phys.* 34, 842−850.

Böhme, H., & Haselkorn, R. (1988) *Mol. Gen. Genet. 214*, 278−285.

Chae, Y. K., Abildgaard, F., Mooberry, E. S., & Markley, J. L. (1994) *Biochemistry 33*, 3287−3295.

Cheng, H., Westler, W. M., Xia, B., Oh, B.-H., & Markley, J. L. (1994) *Arch. Biochem. Biophys.* (in press).

Freeman, R., Kempsell, S. P., & Levitt, M. H. (1980) *J. Magn. Reson.* 38, 453−479.

Ho, K. K., Ulrich, E. L., Krogmann, D. W., & Gomez-Lojero, C. (1979) *Biochim. Biophys. Acta 545*, 236−248.

Holden, H. M., Jacobson, B. L., Hurley, J. K., Tollin, G., Oh, B.-H., Skjeldal, L., Chae, Y. K., Cheng, H., Xia, B., & Markley, J. L. (1994) *J. Bioenerg. Biomembr. 26*, 67−88.

Jacobson, B. L., Chae, Y. K., Böhme, H., Markley, J. L., & Holden, H. M. (1992) *Arch. Biochem. Biophys. 294*, 279−281.

Jacobson, B. L., Chae, Y. K., Markley, J. L., Rayment, I., & Holden, H. M. (1993) *Biochemistry 32*, 6788−6793.

Oh, B.-H., & Markley, (1990) *Biochemistry 29*, 4014−4017.

Rypniewski, W. R., Breiter, D. R., Benning, M. M., Wesenberg, G., Oh, B.-H., Markley, J. L., Rayment, I., & Holden, H. M. (1991) *Biochemistry 30*, 4126−4131.

Vold, R. L., Waugh, J. S., Klein, M. P., & Phelps, D. E. (1968) *J. Chem. Phys.* 48, 3831−3832.

Webb, G. A. (1970) *Annu. Rep. NMR Spectrosc. 3*, 211−259.

BI940930T